DR B. JAYARAM (Orcid ID : 0000-0002-5495-2213)

Article type : Research Article

Non-steroidal Estrogen Receptor Isoform Selective Biphenyls

Seema Bhatnagar[a, #,*], Anjali Soni[b,#], Swati Kaushik[a,c], Megha Rikhi[a], T R Santhosh Kumar[c], B. Jayaram[b,d,*]

[a]*Amity Institute of Biotechnology, Amity University, Noida-201303, India*
[b]*Department of Chemistry and Supercomputing Facility for Bioinformatics & Computational Biology, Indian Institute of Technology, Hauz Khas, New Delhi-110016, India*
[c]*Cancer Research Programme Lab1, Rajiv Gandhi Centre for Biotechnology, Poojappura, Thiruvananthapuram, Kerala- 695014, India*
[d]*Kusuma School of Biological Sciences, Indian Institute of Technology, Hauz Khas, New Delhi-110016, India*
Email: bjayaram@chemistry.iitd.ac.in; sbhatnagar1@amity.edu

*Corresponding authors

[#]Equal contributions

Abstract

Estrogen receptor (ER) has been a therapeutic target to treat ER positive breast cancer, most notably by agents known as selective estrogen receptor modulators (SERMs). However, resistance and severe adverse effects of known drugs gave impetus to the search for newer agents with better therapeutic profile. ERα and ERβ are two isoforms sharing 56% identity, and having different physiological functions and expressions in various tissues. Only two residues differ in the active sites of the two isoforms motivating us to design isoform selective ligands. Guided by computational docking and molecular dynamics simulations, we have designed, synthesized and tested, substituted biphenyl-2,6-diethanones and their derivatives as potential agents targeting ERα. Four of the molecules synthesized exhibited preferential cytotoxicity in ERα+ cell line (MCF-7) compared to ERβ+ cell line (MDA-MB-231). Molecular dynamics (MD) in combination with molecular mechanics-generalized born surface area (MM-GBSA) methods could account for binding selectivity. Further co-treatment and *E-screen* studies with known ER ligands- estradiol (E_2) and tamoxifen (Tam) indicated isoform selective anti-estrogenicity in ERα+ cell line which might be ER mediated. ERα siRNA silencing experiments further confirmed the ER selective nature of ligands.

Introduction

Estrogen Receptor (ER) is the mainstay in breast cancer endocrine therapies[1]. Estrogen plays a critical role in hormone responsive breast cancer progression by binding to ER leading to DNA synthesis and cellular proliferation[2]. The ER isoforms, ERα and ERβ, encoded by separate genes are responsible for mediating estrogen responsive action[3]. ERα is expressed in about 75% of the diagnosed breast tumors

This article has been accepted for publication and undergone full peer review but has not been through the copyediting, typesetting, pagination and proofreading process, which may lead to differences between this version and the Version of Record. Please cite this article as doi: 10.1111/cbdd.13126

and can be treated with agents targeting estrogen mediated signaling[4,5]. One of the most prescribed, first-line adjuvant treatments available for ERα+ breast cancer is tamoxifen, a selective ER modulator[6,7]. Tamoxifen acts as an antagonist in breast tissue but as an agonist in bone and uterus. Contrastingly, its estrogenicity is beneficial in bone to prevent osteoporosis while in uterus, it can lead to endometrial cancer[8]. Moreover, it is observed that tamoxifen responsive breast cancer patients become resistant and long term therapy predisposes them to severe adverse effects such as development of endometrial cancer[9–11]. Besides, signaling through protein kinases also leads to tamoxifen resistance in an estradiol-independent manner[12]. The limited effectiveness of current chemotherapeutic drugs urges identification of some novel ER targeting agents with high efficacy and minimal side effects.

Despite tremendous consistent efforts in this area, ER molecular biology has proven to be exceedingly complex. Though ERs behave as ligand activated transcription factors, ER ligands cannot be considered as 'molecular switches' that activate or deactivate the receptor post ligand binding. It is well established that different ER ligands lead to different ER conformations resulting in agonist, partial agonist, inverse agonist and antagonist behaviors[13].

Nonetheless, identification of potent ER ligands remains a hot area of research providing excellent opportunities for the design of isoform selective agents and is therefore of immediate interest to the drug design community. The ligand binding domain (LBD) of ER isoforms share 56% homology[14]. The dynamic and plastic nature of LBD makes it an attractive target for a wide spectrum of ligands. However in most cases, potent and efficacious ligands are not ER subtype selective; which often translates into off-target toxicity[15,16]. On the contrary, ER subtype selective ligands have suboptimal *in vivo* pharmacokinetics. Extensive studies have been undertaken in the last 50 years to determine critical interacting residues in ER LBD that translate into enhanced potency of ligands. It has been elucidated from previous reports that subtype selective agents must firstly, position substituents close to amino acid differences between ERα and ERβ to develop subtype selectivity; secondly, the ligand must be conformationally rigid; and thirdly, the presence of various substituents including the phenol (or phenolic bioisosteres) can aid in achieving selectivity for ER subtypes through molecular recognition[17–20].

In continuation of our efforts to identify ER subtype selective ligands, we focus here on nonsteroidal scaffolds since nonsteroidal ligands are considered as remarkable high affinity binders against ER[21]. Biphenyl scaffold (Fig. 1) is chosen for designing potential ERα hits, as they could be regarded as surrogates of the steroidal backbone[22]. The current study on biphenyl-2,6-diethanones was undertaken to design and determine key structural determinants in biphenyl scaffold that may confer ERα subtype selectivity.

Methods and Materials

Crystal structures of human ERα and ERβ complexed with 4-hydroxytamoxifen (OHT) and R,R-5,11-cis-diethyl-5,6,11,12-tetrahydrochrysene-2,8-diol (THC) are extracted from RCSB protein data bank with codes 3ERT and 1L2J, respectively[23–25]. Both the complexes have antagonist bound protein conformations. The missing loop regions in 1L2J are modeled using *Modeller*[26]. Biphenyl compounds **3(a-d)** were designed against ERα using structure-based drug design approach[27]. Docking is performed on both the ER isoforms using *ParDOCK* module of *Sanjeevini* software suite developed in-house, which contains built-in features to take care of geometry optimization, partial charge derivation and parameter assignment of the molecules in an automated way[27–29].

To further develop a molecular view of the structure and dynamics of ERα-ligand complexes, molecular dynamics (MD) simulations are carried out. 3ERT is used as ERα control. MD simulations are performed using *AMBER14* software suite on all the docked complexes obtained from *ParDOCK*[30]. Amber 'ff99SB' and 'GAFF' force fields are used for the protein and ligand file preparation. All the simulations are conducted with periodic boundary conditions. The protein-ligand complexes are solvated in a box of TIP3P water molecules and electroneutrality of the system is

maintained[31]. An initial minimization is conducted with 5000 steps (2500SD+2500CG). Simulations are started by slow heating of the solvent to 300 K at constant volume using harmonic restraints of 25 kcal/mol $Å^{-2}$ on the solute atoms for a period of 200ps. These restraints are slowly relaxed to 1 kcal/mol $Å^{-2}$ during equilibration of 1ns. The system is further simulated for production run of 100ns under NPT conditions using Berendsen algorithm with a coupling constant of 5ps[32]. Long-range coulombic interactions are treated using particle mesh ewald method (PME) and a cutoff of 12 Å distance is used for van der Waals (VDW) interactions[33]. Shake is enabled to constrain the covalent bonds involving hydrogens[34].

A detailed analysis of the interaction energies has been carried out using molecular mechanics generalized Born surface area (MM-GBSA) methodology to further provide insights into protein-ligand binding and thus on the inhibitory mechanism of compounds **3(a-d)** against ERα and further to elucidate the basis of specificity of compound **3b** for ERα over ERβ[35,36]. MM-GBSA method employed to predict the binding free energies (ΔG_{bind}) comprises gas phase electrostatics (ELE) and VDW energies, polar and non-polar solvation energies and entropic contributions. 200 snapshots are extracted at equal intervals from the last 10ns stable MD trajectories for binding free energy estimations. For each snapshot, the binding free energy of protein-ligand complex is estimated as:

$$\Delta G_{bind} = G_{complex} - (G_{protein} + G_{ligand}) \quad (1)$$

The ΔG_{bind} is the sum of the changes in molecular mechanics gas-phase binding free energy (ΔG_{MM}), the solvation free energy (ΔG_{solv}) and the entropic contributions ($-T\Delta S$).

$$\Delta G_{bind} = \Delta G_{MM} + \Delta G_{solv} - T\Delta S \quad (2)$$

$$\Delta G_{MM} = \Delta G_{ele} + \Delta G_{vdW} \quad (3)$$

$$\Delta G_{solv} = \Delta G_{pol,solv} + \Delta G_{nonpol,solv} \quad (4)$$

The ELE and VDW (ΔG_{ele} and ΔG_{vdW}) energies are derived from sander as used for MD simulation. The polar contribution to solvation ($\Delta G_{pol,solv}$) is obtained using GBSA module of AMBER14. The non-polar contribution to solvation ($\Delta G_{nonpol,solv}$) is determined using $\Delta G_{nonpol,solv} = \gamma * SASA$, where SASA is the solvent-accessible surface area and γ is the empirical surface tension and is set to 0.0072 kcal/mol-$Å^{-2}$. The conformational entropy contributions to free energies upon ligand binding are calculated using normal-mode analysis by the nmode AMBER module[30]. A total of 200 snapshots are chosen from the last 10ns of MD simulations for the molecular mechanical free energies and solvation energies. However, due to high computational demand for entropy calculations, only 20 snapshots are extracted from the last 10ns of MD trajectories. In addition to MM-GBSA binding free energies, per residue binding free energies are also calculated.

Further, to corroborate the computational findings, the initial set of compounds **1(a-i)** are synthesized by adopting known procedures[37]. The biphenyl derivatives **3(a-d)** are synthesized in two steps from compounds **1(a-b)** as depicted in Fig. 2. In the first step, biphenyl-2,6-diethanone derivatives **1(a-b)** are reacted with NBS in methanol which yielded 1,1'-(3,4'-dihydroxy-5-methylbiphenyl)-2,6-bis-bromodiethanone **2a** and 1,1'-(3,2'-dihydroxy-5-methylbiphenyl)-2,6-bis-bromodiethanone **2b**. In the second step, compounds **2a** and **2b** are further reacted with primary amines, butylamine and 1,4-diaminobutane in presence of acetonitrile/pyridine, yielding the desired products **3(a-d)** (Fig. 2). The structures of compounds are characterized based on their spectroscopic data (^1H, ^{13}C NMR, IR and Mass spectra) as provided in supporting information.

The MTT assay is performed to evaluate the anti-breast activity of all the synthesized compounds against ERα+ (MCF-7) and ERβ+ (MDA-MB-231) cell lines. MRC-5 cell line is used as a control. Followed by, the co-treatment studies are performed with known ER ligands, Tam and E_2.

Protocol adopted is reported by earlier workers[38]. The anti-estrogenicity and antagonist nature of the most active compound is evaluated by *E-screen* assay, where tumor cells are exposed to putative anti-estrogens and cellular proliferation is compared with the tumor cells treated with E_2[39]. The *E-screen* assay is performed in two steps according to the protocol slightly modified from *Soto et al*[40]. Furthermore, the siRNA silencing experiments are performed to confirm ERα selectivity where we silenced ER in ER+ MCF-7 cells using specific siRNA against human ERα. The whole cell extract from silenced and non-silenced cells are prepared to confirm the silencing. The whole cell extract is separated by electrophoresis and western blotting is carried out as described in the supporting information. Further details of all experiments are provided in supporting information.

Results and Discussion

The calculated docking energies of all the four compounds against the active sites of both ER isoforms are shown in Table 1. Reasonably good, preferential docking energies are obtained for most of the biphenyl compounds against ERα but since both isoforms are highly homologous, differing by only two amino acid substitutions in the active sites - Leu384 of ERα is substituted by Met336 in ERβ and Met421 of ERα is substituted by Ile373 in ERβ - the energy differences are small[41]. Docking is also carried out using glide software of Schrodinger and similar results are obtained.

The binding cavity of ERα is mainly comprised of following residues- Arg394, Met421, Glu353, Met343, His524, Ala350, Phe404, Thr347, Leu525, Trp383, Leu384, Ile424 and Gly521. The binding modes of various compounds **3(a-d)** captured from the last stable MD trajectories are shown in Fig. 3. Compound **3a** forms a few nonpolar contacts with His524, Met343, Ala350, Met421 and Met388 with no hydrogen bond formation. Compound **3b** is anchored to the cavity via a hydrogen bond formation between amine group of one of the butylamine derivatives and main chain atoms of Leu525 and capturing almost all the VDW and hydrophobic contacts required for the activity of ERα as depicted in Fig 3. The side chains of compound **3b** make extensive hydrophobic contacts with residues- Met343, Thr347, Ala350, Met388, Phe404, Arg394, Leu391, Met421, Leu346, Leu525 and Trp383. It fits snugly in the cavity of ERα. Compound **3c** forms various hydrogen bonds with Glu353, Leu387, Glu419 and Thr347 with the active site residues of ERα. Its orientation in the cavity is different and therefore forms only a few VDW contacts. Compound **3d** also forms fewer non-polar contacts. Based on these MD derived interaction patterns, we identified compound **3b** to be the most active compound of the biphenyl series **3(a-d)** as it retains some important contacts throughout the simulation as formed by tamoxifen[23].

To assess the dynamic stability of all the complexes during the entire 100ns production MD run, their structural and energetic properties are closely monitored. Root mean square deviations (RMSDs) of compounds **3(a-d)** with ERα backbone in relation to their initial structures are plotted in Fig. S1(a) of supporting information. RMSD tends to converge after 40-50ns indicating the systems stability. RMSD of compound **3b** with ERα and ERβ backbone in comparison to ERα-Tam (3ERT) is plotted in Fig. S1(b) indicating similar RMSD pattern of ERα-**3b** with ERα-Tam and their high stabilities throughout the MD.

The calculated binding free energies (ΔG_{bind}) using MM-GBSA suggest ERα-**3b** complex to be the most stable among the series **3(a-d)** (Table 2). By comparing the energetic contributions of ERα and **3(a-d)**, it is observed that the favorable electrostatics (ΔG_{ele}) are compensated by unfavorable polar solvation energies ($\Delta G_{pol,solv}$) in all the four complexes. The net electrostatic ($\Delta G_{ele}+\Delta G_{pol,solv}$) contributions are unfavorable to binding. The favorable sum of gas phase VDW (ΔG_{vdW}) and nonpolar solvation energies ($\Delta G_{nonpol,solv}$) arising from the ligands hydrophobic core forms the basis of favorable binding energies. The net VDW ($\Delta G_{vdW}+\Delta G_{nonpol,solv}$) values for ERα-**3a**, ERα-**3b**, ERα-**3c** and ERα-**3d** are -64.22, -64.65, -56.75 and -49.92 kcal/mol, respectively. Enthalpic contributions provide the strength of interactions between the receptor and the ligand and entropic contributions provide the change in entropy of the solvent due to ligand binding and loss of conformational degrees of freedom (rotational, vibrational and translational). The unfavorable entropy

contributions in all the systems are opposed by ~23-27 kcal/mol. The net binding free energy comprising enthalpic and entropic terms is higher for ERα-**3b** (-23.63 kcal/mol); dominated by shape complementarity, and thereby resulting in its higher affinity.

To elucidate the selective inhibitory activity of **3b** towards ERα over ERβ, we calculated the MM-GBSA binding free energies for ERβ-**3b** as well. To unravel the selectivity mechanism of **3b**, the binding free energy components of both the complexes ERα-**3b** and ERβ-**3b** are compared. The gas-phase VDW and nonpolar solvation energies are favorable for binding (-64.65 for ERα-**3b** and -66.25 and ERβ-**3b**), but their difference is negligible to account for selectivity. However, the gas-phase electrostatics is playing a subtle role in selectivity of **3b** towards ERα as indicated by the large difference in electrostatic energy of -8.04 kcal/mol (Table 2). Altogether, the enthalpic interactions and the net binding free energies are better for ERα-**3b** explaining its selectivity over ERβ-**3b**.

The important active site residues governing selectivity of **3b** to ERα over (ERβ) are Thr347 (Thr299), Ala350 (Ala302), Trp383 (Trp335), Arg394 (Arg346), Met421 (Ile373), His524 (His475) and Leu525 (Leu476) as shown in Fig. 4. Larger contribution to selectivity is mainly achieved by Thr347 (Thr299), Ala350 (Ala302), Met421 (Ile373) and Leu525 (Leu476). Per-residue energy calculation is also performed on the same 200 snapshots chosen from the last 10ns MD trajectories for MM-GBSA calculations. The relative positions of ligand **3b** in ERα and ERβ are compared with the crystallographic complexes (3ERT and 1L2J) especially with two key residues: Leu384 (Met336) and Met421 (Ile373) shown in Fig. 5. The superposition highlights the orientation of two amino acids which actually differ in ERα (Leu384 and Met421) and ERβ (Met336 and Ile373) resulting in **3b** specificity towards ERα.

Overall, the simulations and the energy analyses strongly point to a preferential binding of **3b** with ERα over ERβ providing a molecular level explanation.

The anti-breast cancer potential of all the synthesized compounds are evaluated against ERα+ (MCF-7) and ERβ+ (MDA-MB-231) cell lines with relevant controls (MRC-5) using MTT assay. The IC_{50} values of compounds **3a, 3b, 3c, 3d** against ERα+ cell line are 62.5, 0.97, 31.25 and 1.95 µg/ml whereas against ERβ+ cell line are >125, 62.5, >125 and 62.5 µg/ml (Fig. 6). The MTT assay measures the cell proliferation rate and conversely, when metabolic events lead to apoptosis or necrosis, the reduction in the cell viability. The MRC-5 cell line is derived from human lung tissue and is used here as control for serving the role of an ER negative cell line. Results for **1(a-i)** are provided in Fig. S2 (supporting information). All the **3(a-d)** compounds exhibit selective inhibitory activity against ERα+ (MCF-7) cell line over ERβ+ (MDA-MB-231). Among them, compound **3b** is found to be the most potent with an IC_{50} value of 0.97 µg/ml (2.27 µM) compared to **3a**, **3c** and **3d** through MTT assay (Fig. 6). MD simulations combined with MM-GBSA and cell line studies suggest compound **3b** as the best representative compound of the series **3(a-d)**, building a strong synergism between computations and experiments. Competitive binding assay could be performed to measure directly the relative binding affinity of compound(s) to ERα, but because of the regulatory issues associated with the use and handling of radioactive compound at our current facility, we could not carry out this work.

In order to determine that the observed anti-proliferative effect of compound **3b** is ER mediated, co-treatment studies are performed to evaluate its synergism with known ER ligands, Tam and E_2. In MCF-7 cell line, our co-treatment results indicate enhanced cytotoxicity when compound **3b** is taken along with Tam and similarly, a reversal effect is observed when compound **3b** is taken with E_2 (Fig. 7). Co-treatment of compound **3b** in MDA-MB-231 and MRC-5, however did not exhibit enhanced cytotoxicity (Fig. S3). Therefore, the co-treatment results exhibited significant synergism of compound **3b** with Tam in ERα+ (MCF-7) cell lines, whereas no synergism was observed in ERβ+ (MDA-MB-231) and ER negative (MRC-5) cell lines, which further indicate that the synergism is directly associated with ERα target and hence affected only ERα+ cell line. Details of co-treatment studies of all the compounds are provided in supporting information.

Time dependent studies with compound **3b** and Tam at IC_{50} concentration in MCF-7 cells also exhibited significant decline in the cell viability (Fig. 8). Altogether, these co-treatment results indicate enhanced cytotoxicity of **3b** in dose and time dependent manner against ERα+ (MCF-7) cell line which plausibly could be ER mediated. These interesting results prompted us to evaluate the anti-estrogenicity of compound **3b**.

Our results from first step (time course studies) of *E-Screen assay* indicate that when MCF-7 cells are exposed to the lowest concentration of E_2 (0.002 µg/ml) along with the range of concentrations of compound **3b** from 24-96 hours, the cytotoxic effects of compound **3b** are significant with a decline in cell viability in a dose and time dependent manner. It is also observed that at concentration 0.48µg/ml, the cytotoxic effect of compound **3b** is abated and a mitogenic response similar to E_2 alone is apparent (Fig. 9(a)). However, as the concentration of compound **3b** is increased, there is a decrease in the cell viability.

Results from second step of *E-screen* assay, when MCF-7 cells are exposed to a range of increasing concentration of E_2 along with IC_{50} concentration of **3b** (0.97µg/ml), show a noticeable effect with increase in MCF-7 cellular proliferation, maximal at 0.013µg/ml (50nM) concentration of E_2 throughout the time period (Fig. 9(b)). The *E-screen* assay results clearly demonstrate that the inhibition of MCF-7 cells induced by compound **3b** can be reversed by the addition of E_2. Since 17β-estradiol has more than 100-fold-greater affinity for ER than Tam, it can compete with Tam or any putative antagonists and restore the receptor processing and other estrogen associated events[38,42].

The above studies indicate that the compound **3b** is selective to ER and its effect on cell proliferation and cell death are subsequent to its ability to target ER. Further we performed siRNA silencing experiments to confirm ERα selectivity of compound **3b**. The specific antibody against ERα is used to detect ERα levels and compared with the house keeping protein β actin (Fig. 10(a)). As shown in the figure, ER has been significantly down regulated in silenced cells compared to parental MCF-7 cells. The parental MCF-7 and silenced cells were exposed to tamoxifen and compound **3b** for 48 hours followed by apoptosis analysis by chromatin condensation as presented in Fig. 10(b) and Fig. 10(c). Silencing of ERα results in a reduction of cell death induced by tamoxifen and **3b**.

Conclusions

In a bid to identify non-steroidal estrogen receptor isoform selective biphenyls, our studies encompassed the use of computational tools for ligand design followed by synthesis and bioactivity evaluation. Our studies indicate that the presence of hydroxyl substituents at *ortho* position of ring B of the biphenyl scaffold (Fig. 1) resulted in compounds **3b** and **3d** exhibiting ERα selectivity. Docking studies indicated that biphenyl compounds containing butylamine groups **3a** and **3b** act as good binders compared to diaminobutane derivatives **3c** and **3d** which act as weak binders. Introduction of long chain substituents on the biphenyl core of ring A in compounds **3(a-d)** resulted in enhanced docking scores indicating better binding affinities with ERα. Further docking and MD studies indicated presence of bulky groups on ring A resulted in non-coplanarity of biphenyl ring which possibly resulted in enhanced docking scores. Analysis of MD results including MM-GBSA suggested **3b** as the best binder with high enthalpic contributions, dominated by van der Waals interactions. The selectivity of **3b** towards ERα over ERβ is dominated by electrostatics and is contributed mainly by back bone atoms of four amino acids residues namely Thr347 (Thr299), Ala350 (Ala302), Met421 (Ile373) and Leu525 (Leu476) as indicated by free energy per-residue decomposition. Cytotoxicity studies of all the compounds belonging to this series indicated higher cytotoxicity in ERα+ cell line (MCF-7) as compared ERβ+ cell line (MDA-MB-231). This is a new finding in the light of reports on 4-hydroxybiphenyl compounds which have 20-70 fold ERβ selectivity[43]. Compound **3b** containing *ortho* hydroxy group was found to be more potent with IC_{50} of 0.97 µg/ml as compared to other compounds. Co-treatment of compound **3b** with known ER antagonist Tam also led to enhanced cytotoxicity which is dose dependent (Fig. 7) and time dependent (Fig. 8). The antagonistic nature of the ligands is confirmed by *E-screen* assay wherein the test compound **3b** is evaluated at IC_{50} concentration in the presence of increasing concentrations of known ER agonist, E_2. The relative proliferative potency (RPP) of compound **3b** as compared to E_2 is

determined to be 0.004. In addition, gene silencing of ER using human siRNA against ER+ MCF-7 cells led to a reduction in cell death induced by compound **3b**. Thus, the results on gene silencing experiments confirmed ERα selectivity of the identified lead **3b** (Fig. 10). The results of our studies could be valuable for future rational design of selective ER inhibitors, providing a better understanding of the energetics of affinity versus selectivity. Results also suggest compound **3b** as a good candidate lead molecule which could be further optimized to explore biphenyl scaffolds in search of better, selective and high affinity ligands.

References

1. Musgrove, E. A & Sutherland, R. L. Biological determinants of endocrine resistance in breast cancer. *Nat. Rev. Cancer* **9,** 631–43 (2009).
2. Hall, J. M., Couse, J. F. & Korach, K. S. The Multifaceted Mechanisms of Estradiol and Estrogen Receptor Signaling. *J. Biol. Chem.* **276,** 36869–36872 (2001).
3. Tsai, M. & O'Malley, B. W. Molecular mechanisms of action of steroid / thyroid receptor superfamily members. *Annu. Rev. Biochem.* **63,** 451–486 (1994).
4. Popolo, A. *et al.* Antiproliferative activity of brown Cuban propolis extract on human breast cancer cells. *Nat Prod Commun* **4,** 1711–1716 (2009).
5. Ali, S. & Coombes, R. C. Endocrine-responsive breast cancer and strategies for combating resistance. *Nat Rev Cancer* **2,** 101–112 (2002).
6. Group, E. B. C. T. C. Relevance of breast cancer hormone receptors and other factors to the efficacy of adjuvant tamoxifen: Patient-level meta-analysis of randomised trials. *Lancet* **378,** 771–784 (2011).
7. Osborne, C. K., Zhao, H. & Fuqua, S. a. Selective estrogen receptor modulators: structure, function, and clinical use. *J. Clin. Oncol.* **18,** 3172–86 (2000).
8. Bernstein, L. *et al.* Tamoxifen Therapy for Breast Cancer and Endometrial Cancer Risk. *JNCI J Natl Cancer Inst* **91,** 1654–1662 (1999).
9. Chang, M. Tamoxifen resistance in breast cancer. *Biomol. Ther. (Seoul).* **20,** 256–67 (2012).
10. Hu, R., Hilakivi-Clarke, L. & Clarke, R. Molecular mechanisms of tamoxifen-associated endometrial cancer (Review). *Oncol. Lett.* **9,** 1495–1501 (2015).
11. Swaby, R. F., Sharma, C. G. N. & Jordan, V. C. SERMs for the treatment and prevention of breast cancer. *Rev. Endocr. Metab. Disord.* **8,** 229–239 (2007).
12. McClaine, R. J., Marshall, A. M., Wagh, P. K. & Waltz, S. E. Ron receptor tyrosine kinase activation confers resistance to tamoxifen in breast cancer cell lines. *Neoplasia* **12,** 650–658 (2010).
13. Heldring, N. *et al.* Estrogen receptors: how do they signal and what are their targets. *Physiol. Rev.* **87,** 905–31 (2007).
14. Dahlman-Wright, K. *et al.* International Union of Pharmacology. LXIV. Estrogen receptors. *Pharmacol. Rev.* **58,** 773–781 (2006).
15. Martinkovich, S., Shah, D., Planey, S. L. & Arnott, J. Selective estrogen receptor modulators: tissue specificity and clinical utility. *Clin. Interv. Aging* **9,** 1437–1452 (2014).
16. Moore, T. W., Mayne, C. G. & Katzenellenbogen, J. A. Minireview: Not Picking Pockets: Nuclear Receptor Alternate-Site Modulators (NRAMs). *Mol. Endocrinol.* **24,** 683–695 (2010).
17. Ng, H. W., Perkins, R., Tong, W. & Hong, H. Versatility or promiscuity: The estrogen receptors, control of ligand selectivity and an update on subtype selective ligands. *Int. J. Environ. Res. Public Health* **11,** 8709–8742 (2014).
18. Paternia, I., Granchia, C., Katzenellenbogen, J. A. & Minutoloa, F. Estrogen Receptors Alpha (ERα) and Beta (ERβ): Subtype Selective Ligands and Clinical Potential. *J.Steroids* **0,** 13–29 (2015).
19. Anstead, G. M., Carlson, K. E. & Katzenellenbogen, J. A. The estradiol pharmacophore: Ligand structure-estrogen receptor binding affinity relationships and a model for the receptor binding site. *Steroids* **62,** 268–303 (1997).
20. Nilsson, S., Koehler, K. F. & Gustafsson, J.-Å. Development of subtype-selective oestrogen receptor-based therapeutics. *Nat. Rev. Drug Discov.* **10,** 778–792 (2011).
21. Gao, H., Katzenellenbogen, J. a, Garg, R. & Hansch, C. Comparative QSAR analysis of

estrogen receptor ligands. *Chem. Rev.* **99,** 723–44 (1999).
22. Lesuisse, D. *et al.* Biphenyls as surrogates of the steroidal backbone. Part 1: synthesis and estrogen receptor affinity of an original series of polysubstituted biphenyls. *Bioorg. Med. Chem. Lett.* **11,** 1709–1712 (2001).
23. Shiau, A. K. *et al.* The structural basis of estrogen receptor/coactivator recognition and the antagonism of this interaction by tamoxifen. *Cell* **95,** 927–937 (1998).
24. Shiau, A. K. *et al.* Structural characterization of a subtype-selective ligand reveals a novel mode of estrogen receptor antagonism. *Nat. Struct. Biol.* **9,** 359–64 (2002).
25. Berman, H. M. *et al.* The Protein Data Bank. *Nucleic Acids Res.* **28,** 235–242 (2000).
26. Fiser, a *et al.* Modeling of loops in protein structures. *Protein Sci.* **9,** 1753–73 (2000).
27. Jayaram, B. *et al.* Sanjeevini: a freely accessible web-server for target directed lead molecule discovery. *BMC Bioinformatics* **13 Suppl 1,** S7 (2012).
28. Jain, T. & Jayaram, B. An all atom energy based computational protocol for predicting binding affinities of protein-ligand complexes. *FEBS Lett.* **579,** 6659–6666 (2005).
29. Gupta, a, Gandhimathi, a, Sharma, P. & Jayaram, B. ParDOCK: an all atom energy based Monte Carlo docking protocol for protein-ligand complexes. *Protein Pept. Lett.* **14,** 632–646 (2007).
30. Case, D. A. *et al.* The Amber biomolecular simulation programs. *Journal of Computational Chemistry* **26,** 1668–1688 (2005).
31. Jorgensen, W. L., Chandrasekhar, J., Madura, J. D., Impey, R. W. & Klein, M. L. Comparison of simple potential functions for simulating liquid water. *J. Chem. Phys.* **79,** 926 (1983).
32. Berendsen, H. J. C., Postma, J. P. M., van Gunsteren, W. F., DiNola, a & Haak, J. R. Molecular dynamics with coupling to an external bath. *J. Chem. Phys.* **81,** 3684–3690 (1984).
33. Essmann, U. *et al.* A smooth particle mesh Ewald method. *J Chem Phys* **103,** 8577–8593 (1995).
34. Ryckaert, J. P., Ciccotti, G. & Berendsen, H. J. C. Numerical integration of the cartesian equations of motion of a system with constraints: molecular dynamics of n-alkanes. *J. Comput. Phys.* **23,** 327–341 (1977).
35. Gohlke, H., Kiel, C. & Case, D. A. Insights into Protein–Protein Binding by Binding Free Energy Calculation and Free Energy Decomposition for the Ras–Raf and Ras–RalGDS Complexes. *J. Mol. Biol.* **330,** 891–913 (2003).
36. Kalra, P., Reddy, T. V. & Jayaram, B. Free energy component analysis for drug design: A case study of HIV-1 protease-inhibitor binding. *J. Med. Chem.* **44,** 4325–4338 (2001).
37. Sharma, A., Pandey, J. & Tripathi, R. P. An efficient regioselective synthesis of functionalized biphenyls via sequential reactions of aromatic aldehydes and β-keto esters or ketones. *Tetrahedron Lett.* **50,** 1812–1816 (2009).
38. Lewis, J. B. *et al.* 4-Hydroxytamoxifen-induced cytotoxicity and bisphenol A: competition for estrogen receptors in human breast cancer cell lines. *In Vitro Cell. Dev. Biol. Anim.* **36,** 320–6 (2000).
39. Soto, A. M.; Lin, T. M.; Justicia, H.; Silvia, R. M.; Sonnenschein, C. in *Chemically induced alterations in sexual and functional development; the wildlife/human connection* (ed. Colborn T, C. C.) 295–309 (NJ: Princeton Scientific Publishing, 1992).
40. Chow, S. Suppression of cell proliferation and regulation of estrogen receptor alpha signaling pathway by arsenic trioxide on human breast cancer MCF-7 cells. *J. Endocrinol.* **182,** 325–337 (2004).
41. Pike, a C. *et al.* Structure of the ligand-binding domain of oestrogen receptor beta in the presence of a partial agonist and a full antagonist. *EMBO J.* **18,** 4608–4618 (1999).
42. Chen, H., Clemens, T. L., Hewison, M. & Adams, J. S. Estradiol and tamoxifen mediate rescue of the dominant-negative effects of estrogen response element-binding protein in vivo and in vitro. *Endocrinology* **150,** 2429–2435 (2009).
43. Edsall, R. J., Harris, H. A., Manas, E. S. & Mewshaw, R. E. ERβ ligands. Part 1: The discovery of ERβ selective ligands which embrace the 4-hydroxy-biphenyl template. *Bioorganic Med. Chem.* **11,** 3457–3474 (2003).

Acknowledgements
The authors gratefully acknowledge Amity University for infrastructure and facilities. Author, MR thanks financial assistance through Amity Science, Technology and Innovation Foundation (ASTIF) fellowship provided by Amity University.-Support to the Supercomputing Facility for Bioinformatics & Computational Biology (SCFBio), IIT Delhi from the Department of Biotechnology, Govt. of India is gratefully acknowledged. The authors also acknowledge the support from Cancer Research Programme Lab 1, Rajiv Gandhi Centre for Biotechnology (RGCB).

Author's contributions
AS performed computational studies. MR performed the synthesis and biological activities. SK and TRSK performed ER siRNA silencing experiments. SB, BJ designed the project. All authors analyzed the results and wrote the manuscript.
Corresponding Author
*E-mail: sbhatnagar1@amity.edu; bjayaram@chemistry.iitd.ac.in

Competing financial interests
The authors declare no competing financial interests.

Supporting information available
The supporting information contains the detail of experimental procedures for organic synthesis, bioactivity assays, spectroscopic characterization of compounds and anticancer activity of **1(a-i)** and **3(a-d)**.

Figure and Table captions

Figure 1: Compounds of interest

Figure 2: Synthesis of biphenyl-2,6-diethanone derivatives.

Figure 3: A comparative depiction of interactions of biphenyl compounds **3(a-d)** with the active site residues of ERα. The violet color represents various biphenyl compounds. Dashed bonds represent the hydrogen bonds along with the distances whereas arcs represent VDW and hydrophobic contacts. Circled residues represent hydrophobic side chain interactions with the corresponding ligands which are also observed in ERα complexed with tamoxifen. All the snapshots for the above analyses are taken from the last 10ns of the MD trajectories.

Figure 4: A comparison of per-residue binding free energy for key residues between ERα-**3b** and ERβ-**3b**.

Figure 5: **(a)** A superposition of complex ERα-**3b** (cyan) with ERα-Tam (pdb id: 3ERT) (magenta). **(b)** A superposition of complex ERβ-**3b** (cyan) with ERβ-THC (pdb id: 1L2J) (magenta). For clarity all hydrogens are removed and only a few important amino acids interactions are displayed to highlight selectivity. Yellow dotted bonds represent hydrogen bonds.

Figure 6: Dose dependent studies of biphenyl-2,6-diethanone derivatives **3(a-d)** plotted against optical density (OD) at 570nm in MCF-7, MDA-MB-231 and MRC-5 cell lines using MTT assay. The data are means and standard error of the mean (SEM) from three samples of each group. Two-way ANOVA followed by Bonferroni post test where p-value < 0.05 is significant for compounds.

Figure 7: Results of co-treatment studies at varied concentrations of compound **3b** alone and in combination with Tam against MCF-7 cell line. All the concentrations are in µg/ml.

Figure 8: Time course of the effect of combination of 0.056 µg/ml Tam and 0.97 µg/ml **3b** on MCF-7 cells. Mitochondrial dehydrogenase activity is measured via MTT assay for the selected time period.

Cells with media are considered as negative control and with 0.002 µg/ml (10nM) E_2 as positive control.

Figure 9: **(a)** Time course of the effect of treatment with 0.002µg/ml (10nM) E_2 and a range of concentration of **3b** on mitochondrial dehydrogenase activity of the MCF-7 cells; **(b)**: Time course of the effect of co-treatment with 0.97µg/ml (2.27µM) **3b** and a range of concentrations of E_2 on mitochondrial dehydrogenase activity of the MCF-7 cells to establish estrogen rescue phenomena. All the concentration units are µg/ml.

Figure 10: **(a)** Gene silencing experiment. Expression of ERα protein by western blot analysis following transfection with ERα siRNA. The difference in the expression of ERα in silenced as compared to parent MCF-7 cells is shown. **(b)** Effect of tamoxifen and **3b** on induction of apoptosis in parental and silenced cells. Parental and ERα silenced MCF-7 cells are assessed for nuclear condensation following 48 hours treatment with tamoxifen (5.63 µg/ml) and **3b** (15, 31.25, 62.5, 125, 250 µg/ml) by Hoechst staining. **(c)** Data is expressed as Mean±STD of nuclear condensation expressed as a percentage (n=3) (*P<0.001).

Table 1: Calculated binding free energies (in kcal/mol) for ERα and ERβ with compounds **3(a-d)** using *ParDOCK*

Table 2: Binding free energies (kcal/mol) calculated using MM-GBSA method for ERα and ERβ

Biphenyl compounds	**ERα (3ERT)**	**ERβ (1L2J)**
3a	-8.00	-7.67
3b	-7.50	-7.43
3c	-6.81	-6.48
3d	-6.01	-5.46

Table 2: Binding free energies (kcal/mol) calculated using MM-GBSA method for ERα and ERβ.

Terms	ERα-3a	ERα-3b	ERα-3c	ERα-3d	ERβ-3b
ΔG_{ele}	-7.20 (3.68)	-16.44 (4.37)	-54.11 (12.59)	-14.97 (5.93)	-8.40 (4.20)
ΔG_{vdW}	-56.15 (3.24)	-57.13 (3.47)	-50.61 (3.89)	-43.77 (3.09)	-58.39 (2.68)
$\Delta G_{pol,solv}$	30.91 (3.36)	33.39 (3.31)	62.49 (8.71)	36.45 (4.54)	28.20 (2.33)
$\Delta G_{nonpol,solv}$	-8.07 (0.33)	-7.52 (0.44)	-7.64 (0.29)	-6.15 (0.39)	-7.86 (0.27)
$\Delta G_{ele}+\Delta G_{pol,solv}$	23.71	16.95	8.38	21.48	19.8
$\Delta G_{vdW}+\Delta G_{nonpol,solv}$	-64.22	-64.65	-56.75	-49.92	-66.25
ΔH	-40.51 (3.21)	-47.71 (3.82)	-49.87 (5.07)	-28.45 (3.64)	-46.46 (3.41)
$T\Delta S$	-23.64 (3.24)	-24.08 (4.84)	-27.35 (4.53)	-23.36 (4.01)	-26.05 (5.32)
ΔG_{bind}	-16.87 (4.98)	-23.63 (4.72)	-22.52 (6.21)	-5.09 (6.06)	-20.41 (5.81)

* Standard deviations (STD) are displayed in parentheses.

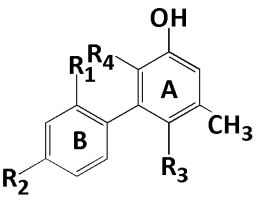

Biphenyl Scaffold

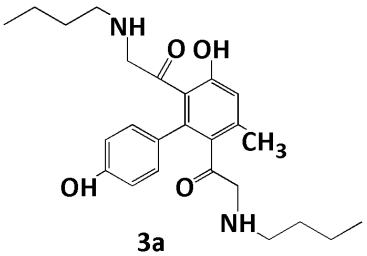

3a

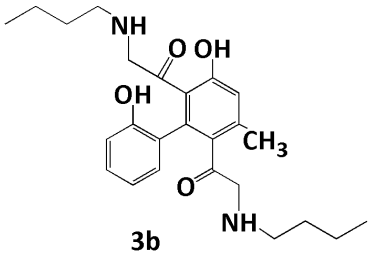

3b

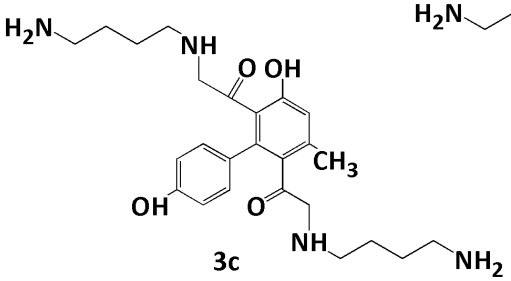

3c

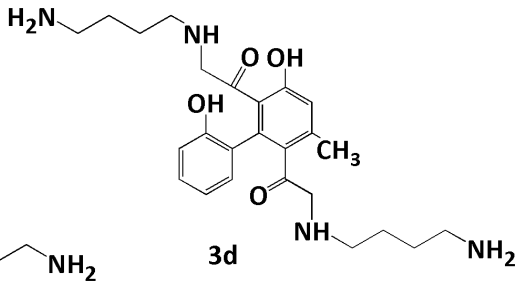

3d

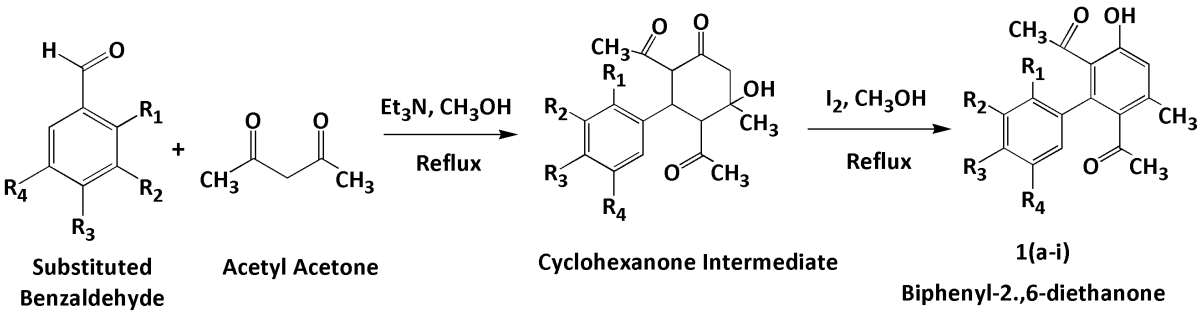

Substituted Benzaldehyde

Acetyl Acetone

Cyclohexanone Intermediate

1(a-i)

Biphenyl-2.,6-diethanone

Where

a) $R_1=R_2=R_4=H$, $R_3=OH$; b) $R_1=OH$, $R_2=R_3=R_4=H$;c) $R_1=R_2=R_3=R_4=H$;

d) $R_1=R_2=R_4=H$, $R_3=OCH3$; e) $R_1=OH$, $R_2=Cl$, $R_3=R_4=H$; f) $R_1=OH$, $R_2=CH3$, $R_3=R_4=H$;

g) $R_1=OH$, $R_2=R_3=H$, $R_4=Cl$; h) $R_1=R_2=R_4=H$, $R_3=N(CH3)2$; i) $R_1=OH$, $R_2=R_3=H$, $R_4=CH3$

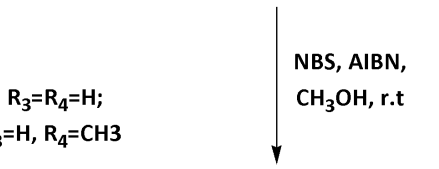

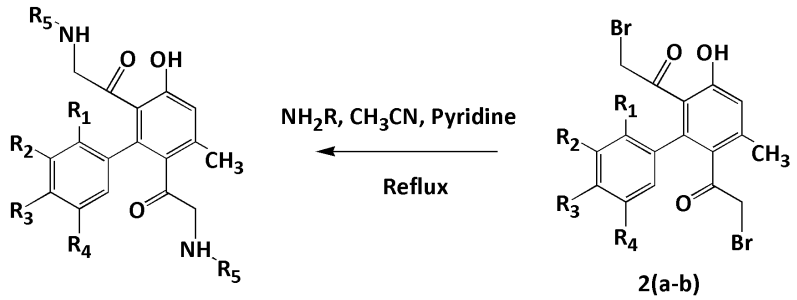

2(a-b)

Biphenyl-2.,6-bis-bromodiethanone

3(a-d)

Where

3a) $R_1=R_2=R_4=H$, $R_3=OH$, $R_5=(CH2)3-CH3$;

3b) $R_1=OH$, $R_2=R_3=R_4=H$, $R_5=(CH2)3-CH3$;

3c) $R_1=R_2=R_4=H$, $R_3=OH$, $R_5=(CH2)4-NH2$;

3d) $R_1=OH$, $R_2=R_3=R_4=H$, $R_5=(CH2)4-NH2$